in vivo *25*: 603-608 (2011)

Subcutenous Xenografts of Human T-Lineage Acute Lymphoblastic Leukemia Jurkat Cells in Nude Mice

ROMAN MEZENCEV and JOHN F. MCDONALD

Georgia Institute of Technology, School of Biology, Atlanta, GA 30332, U.S.A.

Abstract. *Background: Human T-acute lymphoblastic leukemia (T-ALL) Jurkat cells are often used for in vitro screening of anticancer compounds; however, in vivo models employing Jurkat cells have not yet been sufficiently described. In this report, the growth characteristics and histology of tumor masses developed following subcutaneous (s.c.) implantation of Jurkat cells into nude mice are presented. Materials and Methods: Five million Jurkat cells in Matrigel™ were injected s.c. into female CrTac:Ncr-Foxn1^{nu} mice. Serial tumor volumes were determined and tumor sections were stained with hematoxylin/eosin and examined histologically. Results: Tumors developed in 86.4% of the mice at a median of 39 days post-implantation. Tumor regressions and small stationary tumors were observed in 47.4% of the tumor-bearing animals. The remaining animals displayed progressive tumor growth reaching a volume of 1000 mm^3 at median day 48 post-implantation. The tumor histology was consistent with lymphoblastic lymphoma. Conclusion: Due to frequent spontaneous regressions, this model is not appropriate for evaluation of T-ALL targeting therapeutics.*

Acute lymphoblastic leukemia (ALL) is the most prevalent type of leukemia in children, as well as being the most common pediatric malignancy. About 15% of pediatric patients express T-lineage-associated antigens, and T-ALL is associated with numerous unfavorable presenting characteristics and a worse prognosis compared to B-lineage ALL. Moreover, to achieve comparable therapeutic outcome, patients with T-ALL generally require more aggressive therapy than B-ALL patients and only a very small proportion of patients with relapsed T-ALL can be cured with combined high-dose chemotherapy and radiotherapy followed by bone marrow transplantation (1). For this reason, the development of new therapeutics that target T-ALL or alter their response to chemo- and radiotherapy is warranted.

The Jurkat T-leukemia cell line, originally established from peripheral blood of a 14-year-old boy with relapsed ALL (2), has been widely used for *in vitro* screening of prospective cancer therapeutics (3-6), including high throughput screening of anticancer agents (7, 8). However, the use of animal models employing Jurkat cells has been reported only rarely (9-12) and the few reported murine models varied substantially in many characteristics. In order to develop an appropriate model for *in vivo* validation of agents active against Jurkat cells *in vitro*, the utility of a murine model using subcutaneously (*s.c.*) xenografted Jurkat cells in nude mice was investigated. Here the growth characteristics and histology of solid tumor masses formed in this model are reported, and the potential of the model for *in vivo* validation of anticancer agents is evaluated.

Materials and Methods

Cell culture. Acute T-lymphoblastic leukemia Jurkat cells, clone E6-1, were obtained from the American Type Culture Collection (Manassas, VA, USA; ATCC No. TIB-152™) and maintained in RPMI 1640 medium supplemented with fetal bovine serum (10%), L-glutamine (2 mM), penicillin (100 IU/mL), streptomycin (100 μg/mL) and amphotericin B (0.25 μg/mL) in an atmosphere of humidified air with 5% CO_2. Cells from exponentially growing culture in passage 6 were washed twice with PBS, pelleted and mixed with Matrigel™. The Jurkat cells used in this experiment were examined for the presence of rodent and human viral pathogens using the Infectious Microbe PCR Amplification Test (IMPACT II and h-IMPACT) and all results were negative (MU Research Animal Diagnostic Laboratory, Columbia, MO, USA).

Animals. Female nude mice, *CrTac:Ncr-Foxn1^{nu}* (Taconic, Hudson, NY, USA) were housed in sterile, filter-capped Microisolator™ cages (Lab Products, Seaford, DE, USA) on a 12-h light/dark cycle and allowed sterile water and 7912 (Harlan Teklad Laboratory Animal Diets and Bedding, Madison, WI, USA) irradiated rodent diet *ad libitum*. All the animal experiments were approved by the Institutional Animal Care and Use Committee (IACUC) and carried out in compliance with the Public Health Service (PHS) Policy on Humane

Correspondence to: Roman Mezencev, Georgia Institute of Technology, School of Biology, 310 Ferst Dr, Atlanta, GA 30332, U.S.A. Tel: +1 4043856628, Fax: +1 4048940519, e-mail: roman.mezencev@biology.gatech.edu

Key Words: Jurkat cells, leukemia, lymphoblastic lymphoma, nude mice, T-acute lymphoblastic leukemia, tumor xenograft.

Care and Use of Animals and the Institute for Laboratory Animal Research (ILAR) Guide for the Care and Use of Laboratory Animals.

Xenografting. Five million Jurkat cells in 100 μL of BD Matrigel™ (basement membrane matrix, growth factor reduced, phenol red-free, BD, Franklin Lakes, NJ, USA, Cat. No. 356231) were injected subcutaneously into the flank region of 6-week-old mice. Tumor volumes (V) were estimated at least twice per week from vernier caliper measurements of perpendicular length (L) and width (W) and calculated as: $V=(\pi/6)\times L\times W^2$ (13). The animals were followed for up to 80 days post-implantation or until they met any study end-point. Tumor-related end-points included: tumor volume >1500 mm^3; largest tumor dimension >15 mm; skin lesions present over tumor; body condition score 1 (14), and weight loss greater than 10%. For the evaluation of tumor growth, individual xenografts were classified as follow: no-take: tumor could not be seen or palpated within 80 days; spontaneous regression: tumor volume decreased to at least 50% of its maximum volume; stationary tumor: tumor volume maintained a size of ≤500 mm^3 or decreased by less than 50% within 80 days and progressive tumor: tumor volume steadily increased above 500 mm^3 within 80 days. Animals that met the study end-points were immediately euthanized; the spleen, lung liver, kidney and tumor tissues were harvested, formalin-fixed and paraffin-embedded, and 5 μm sections were cut and stained with hematoxylin/eosin (H/E).

Results

Tumor growth was observed in 19 implanted mice (take rate 86.4%) with median time to detectable tumors of 39 days (range 30-53 days, Figure 1, TTT). Tumor regressions and stationary tumors were observed in 6 and 3 mice, respectively (31.6% and 15.8% of the tumor-bearing animals). Complete spontaneous regression was observed in small tumors with maximum volume ≤288 mm^3 and tumors exceeding this volume tended to grow progressively. One partial spontaneous regression was observed in an advanced tumor that reached a volume of 980 mm^3. Similarly, stationary tumors were small with maximum volume ≤268 mm^3 (Figure 2). Ten mice (52.6% of the tumor-bearing animals) displayed progressively growing tumors and had to be euthanized due to tumor-related end-points at median 49 days post-implantation (range 41-70, Figure 1, TTE). In animals with progressively growing tumors, advanced stage tumors with V ≥1000 mm^3 were reached at a median of 48 days post-injection (range 38-70 days, Figure 1, TTA).

Macroscopically, tumors presented as soft yellowish masses with a smooth surface, visible vascularization, sometimes with a central cavity and areas of hemorrhage (Figure 3). H/E-stained tumor sections demonstrated monomorphic sheets of lymphoblasts with no architectural pattern, broken by focal 'starry sky' appearance (macrophages phagocytosing apoptotic cells), prominent areas of necrosis and extension into adjacent fat tissue. Neoplastic cells had scant cytoplasm and round, occasionally convoluted, nuclei with finely stippled chromatin, inconspicuous nucleoli and displayed a high mitotic rate (Figure 4). Although the histological findings in the tumor sections were consistent with lymphoblastic lymphoma, no leukemic infiltrations were detected in the liver, lungs, spleen or kidneys.

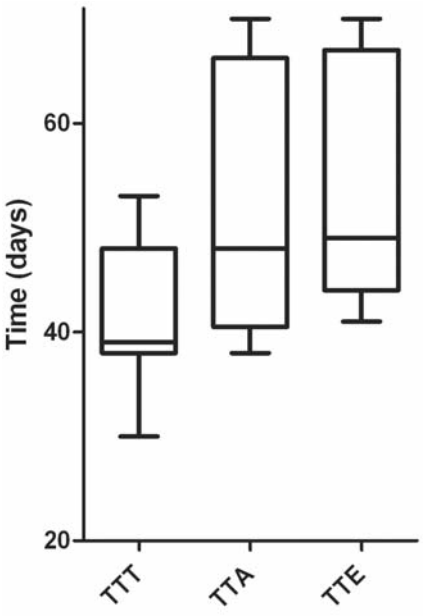

Figure 1. *Box-and-whisker plots depicting distributions of time to visible tumor (TTT), time to advanced tumor ≥1000 mm^3 (TTA) and time to tumor-burden-related euthanasia (TTE) post s.c. implantation of Jurkat cells. Each plot presents (from the bottom) shortest observation, lower quartile, median, upper quartile and longest observation.*

Discussion

Waurzyniak and Schneider (15) have previously used an animal model of human T-ALL based on intravenous (*i.v.*) inoculation of 10^7 MOLT-3 cells into severe combined immunodeficient (SCID) mice and demonstrated *in vivo* therapeutic efficacy of a cluster of differentiation 7 (CD-7)-targeted immunotoxin. That model employed death/survival as an experimental end-point, with untreated animals dying at median day 37 post-injection due to systemic disease with the formation of subcutaneous and abdominal tumor masses and leukemic infiltration of bone marrow, brain, kidneys, liver, lungs, lymph nodes, skeletal muscles, spleen, thymus and adrenal glands (15).

For reasons of animal welfare, *in vivo* models with end-points other than death due to the disease are currently preferred. In this context, subcutaneous xenografts from human tumor cell lines provide the benefit of serial determination of tumor volumes with calipers and selection of tumor volume as a humane study end-point. The Developmental Therapeutic Program of the National Cancer Institute (DTP/NCI) operates

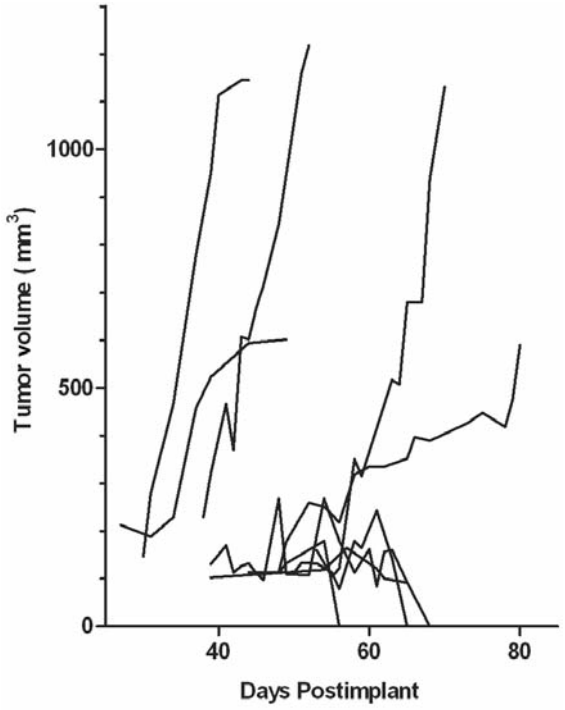

Figure 2. *Growth curves of 9 representative tumors from s.c. implanted Jurkat cells demonstrating progressive growth, spontaneous regressions and stationary growth.*

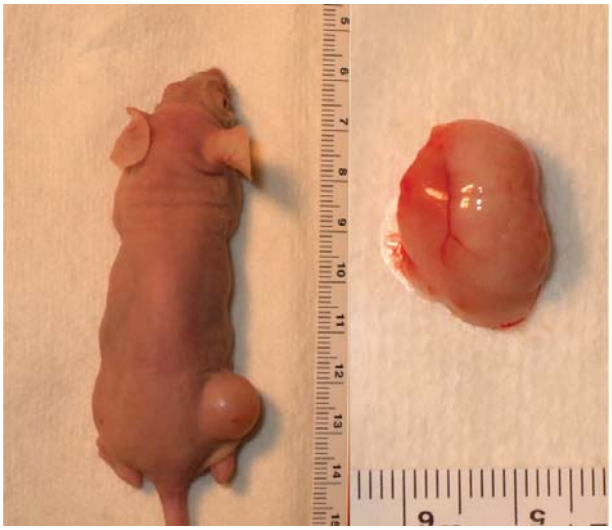

Figure 3. *Nude mouse with advanced tumor following s.c. implantation of Jurkat T-ALL cells (left). Macroscopic appearance of tumor nodule with smooth surface and visible vascularization (right).*

an anticancer compound screening program that includes the use of human T-ALL cell lines MOLT-4 and CCRF-CEM, but not Jurkat, growing subcutaneously in nude mice, with take rates of 80-100% and 60-80%, respectively (16). A subcutaneous Jurkat xenograft tumor model was previously established in γ-irradiated triple-deficient immunocompromised beige nude mice NIH/bg/nu/xid after injection of 2.5×10^7 Jurkat cells along with irradiated HT-1080 human sarcoma feeder cells, with tumor nodules visible by day 7 and no spontaneous regressions (10). Jurkat cell *s.c.* xenografts in nude (*nu/nu*) mice were reportedly established after injection of 5×10^6 Jurkat cells in 100 μL of Matrigel™ with tumor nodes palpable within 2 weeks (9), which was sooner than in the present experiment. Fujita *et al.* (11) reported a Jurkat model established in *nu/nu* mice with tumors observed 8 weeks after injections in 20%, 80% and 100% of mice after *s.c.* injection of 10^6, 10^7 and 10^8 cells in PBS, respectively. The present 86.4% take rate with detectable tumors at a median of 39 days post-injection was not inconsistent with this report, considering the fact that Matrigel™ can increase tumor growth and/or malignant potential of xenogeneic tumor cells (17).

However, as well as an acceptable take rate, a high proportion of spontaneous tumor regressions and formation of small stationary tumors also occurred in the present study. Furthermore, subcutaneous tumors that require more than 21 days to reach a tumor burden of 1000 mm^3/mouse are considered unacceptable for primary screening at DTP/NCI due to high mouse-to-mouse variability (18). As a result, the Jurkat cell *s.c.* xenograft in nude mice is not an appropriate model for evaluation of T-ALL targeted therapeutics. Spontaneous tumor regressions are probably a consequence of an immunogenic problem with a tumor model and suggest the effect of residual immune response of nude mice to Jurkat cell xenograft. Consequently, non-obese diabetic (NOD)/SCID mice that are less immunocompetent than nude and SCID mice due to defects in natural killer (NK) cells, complement and macrophage function, may be a more appropriate host for a *s.c.* Jurkat xenograft tumor model.

Acknowledgements

This work was supported by The Ovarian Cancer Institute, The Ovarian Cycle Foundation, The Robinson Family Foundation, The Deborah Nash Harris Endowment Fund, The Watefall Foundation and OBNET Women's Healthcare. The Authors thank Dr. DeEtte Walkes for reviewing the manuscript.

References

1 Uckun FM, Sensel MG, Sun L, Steinherz PG, Trigg ME, Heerema NA, Sather HN, Reaman GH and Gaynon PS: Biology and treatment of childhood T-lineage acute lymphoblastic leukemia. Blood *91(3)*: 735-746, 1998.

2 Schneider U, Schwenk HU and Bornkamm G: Characterization of EBV-genome negative 'null' and 'T' cell lines derived from children with acute lymphoblastic leukemia and leukemic transformed non-Hodgkin lymphoma. Int J Cancer *19(5)*: 621-626, 1977.

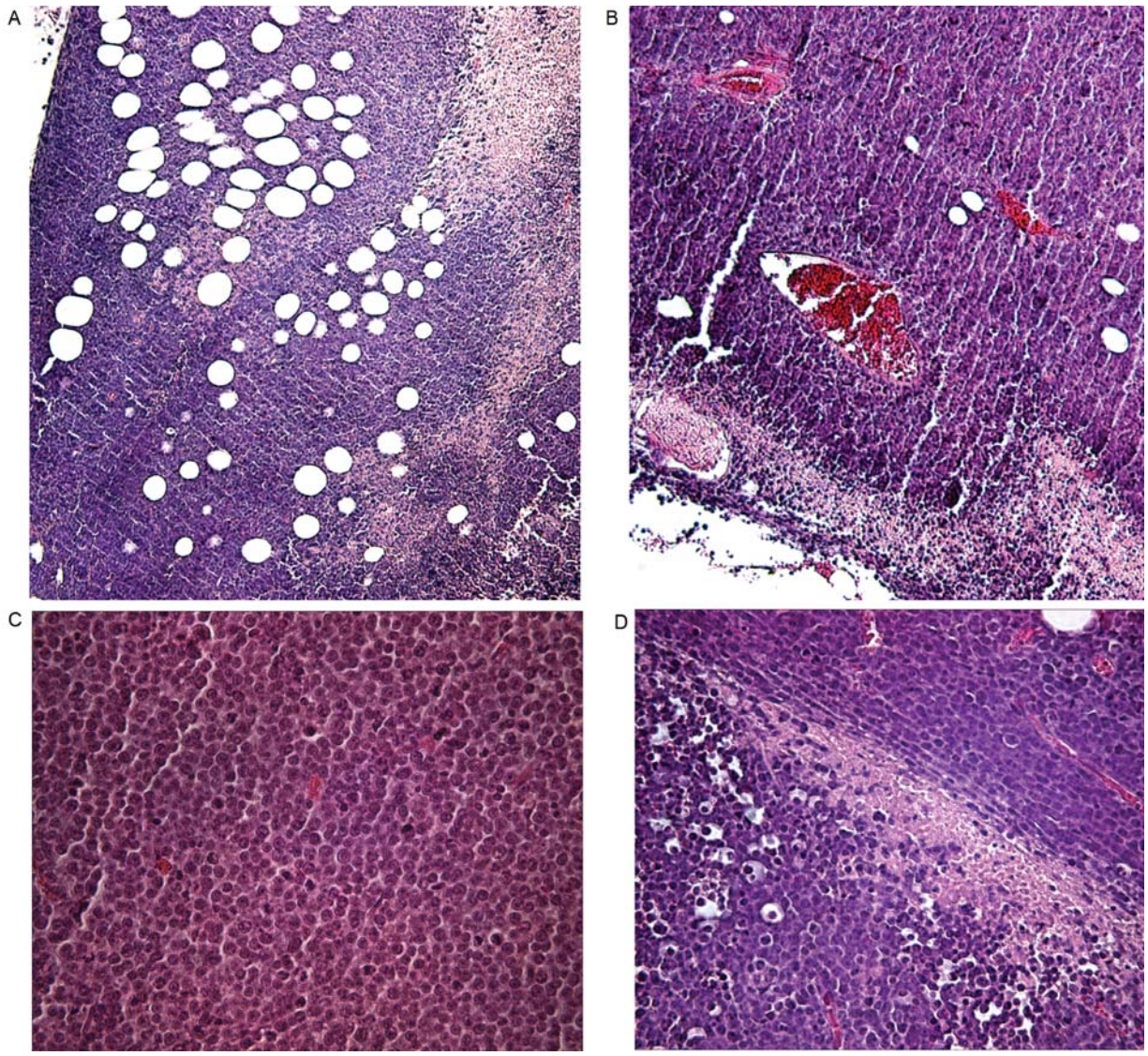

Figure 4. *H/E-stained tumor sections. Monomorphic sheets of malignant lymphoblasts with no architectural pattern (A-D); peritumoral fat tissue invasion (A, B); vascularization (B); focal 'starry sky' appearance (D), prominent areas of necrosis (A, B, D), neoplastic lymphoblasts with scant cytoplasm, finely strippled chromatin and high mitotic rate (C). Magnification: A and B (×100), C (×400), D (×200).*

3 Chiarini F, Grimaldi C, Ricci F, Tazzari PL, Evangelisti C, Ognibene A, Battistelli M, Falcieri E, Melchionda F, Pession A, Pagliaro P, McCubrey JA and Martelli AM: Activity of the novel dual phosphatidylinositol 3-kinase/mammalian target of rapamycin inhibitor NVP-BEZ235 against T-cell acute lymphoblastic leukemia. Cancer Res *70(20)*: 8097-8107, 2010.

4 Youns M, Fu YJ, Zu YG, Kramer A, Konkimalla VB, Radlwimmer B, Sültmann H and Efferth T: Sensitivity and resistance towards isoliquiritigenin, doxorubicin and methotrexate in T-cell acute lymphoblastic leukaemia cell lines by pharmacogenomics. Naunyn Schmiedebergs Arch Pharmacol *382(3)*: 221-234, 2010.

5 Romagnoli R, Baraldi PG, Cruz-Lopez O, Lopez Cara C, Carrion MD, Brancale A, Hamel E, Chen L, Bortolozzi R, Basso G and Viola G: Synthesis and antitumor activity of 1,5-disubstituted 1,2,4-triazoles as *cis*-restricted combretastatin analogues. J Med Chem *53(10)*: 4248-4258, 2010.

6 dos Santos MP, Schwartsmann G, Roesler R, Brunetto AL and Abujamra AL: Sodium butyrate enhances the cytotoxic effect of antineoplastic drugs in human lymphoblastic T-cells. Leuk Res *33(2)*: 218-221, 2009.

7 Kemnitzer W, Drewe J, Jiang S, Zhang H, Wang Y, Zhao J, Jia S, Herich J, Labreque D, Storer R, Meerovitch K, Bouffard D, Rej R, Denis R, Blais C, Lamothe S, Attardo G, Gourdeau H, Tseng B, Kasibhatla S and Cai SX: Discovery of 4-aryl-4*H*-chromenes as a new series of apoptosis inducers using a cell- and caspase-based high-throughput screening assay. 1. Structure–activity relationships of the 4-aryl group. J Med Chem *47(25)*: 6299-6310, 2004.

8 Townsend JB, Shaheen F, Liu R and Lam KS: Jeffamine derivatized TentaGel beads and poly(dimethylsiloxane) microbead cassettes for ultrahigh-throughput *in situ* releasable solution-phase cell-based screening of one-bead–one-compound combinatorial small molecule libraries. J Comb Chem *12(5)*: 700-712, 2010.
9 Ponomarev V, Doubrovin M, Lyddane C, Beresten T, Balatoni J, Bornman W, Finn R, Akhurst T, Larson S, Blasberg R, Sadelain M and Tjuvajev JG: Imaging TCR-dependent NFAT-mediated T-cell activation with positron-emission tomography *in vivo*. Neoplasia *3(6)*: 480-488, 2001.
10 Neville DM Jr, Scharff J and Srinivasachar K: *In vivo* T-cell ablation by a holo-immunotoxin directed at human CD3. Proc Natl Acad Sci USA *89(7)*: 2585-2589, 1992.
11 Fujita K, Tsujimura A, Hirai T, Ohta H, Matsuoka Y, Miyagawa Y, Takao T, Takada S, Nonomura N and Okuyama A: Effect of human leukemia cells in testicular tissues grafted into immunodeficient mice. Int J Urol *15(8)*: 733-738, 2008.
12 Arai M, Koizumi Y, Sato H, Kawabe T, Suganuma M, Kobayashi H, Tomoda H and Omura S: Boromycin abrogates bleomycin-induced G_2 checkpoint. J Antibiot (Tokyo) *57(10)*: 662-668, 2004.
13 Norton L and Simon R: New thoughts on the relationship of tumor growth characteristics to sensitivity to treatment. *In*: Methods in Cancer Research. Vol. XVII, Part B. DeVita V and Busch H (eds.) Academic Press, New York, pp. 53-90, 1979.
14 Ullman-Culleré MH and Foltz CJ: Body condition scoring: a rapid and accurate method for assessing health status in mice. Lab Anim Sci *49(3)*: 319-323, 1999.
15 Waurzyniak B, Schneider EA, Tumer N, Yanishevski Y, Gunther R, Chelstrom LM, Wendorf H, Myers DE, Irvin JD, Messinger Y, Ek O, Zeren T, Langlie MC, Evans WE and Uckun FM: *In vivo* toxicity, pharmacokinetics, and antileukemic activity of TXU (anti-CD7)-pokeweed antiviral protein immunotoxin. Clin Cancer Res *3(6)*: 881-890, 1997.
16 Plowman J, Dykes DJ, Hollingshead M, Simpson-Herren L and Alley MC: Human tumor xenograft models in NCI drug development. *In*: Anticancer Drug Development Guide. Teicher BA (ed.). Humana Press, Totowa, NJ, pp. 101-125, 1997.
17 Topley P, Jenkins DC, Jessup EA and Stables JN: Effect of reconstituted basement membrane components on the growth of a panel of human tumour cell lines in nude mice. Br J Cancer *67(5)*: 953-958, 1993.
18 Corbett T, LoRusso P, Panchapor C, White K, Demchik L and Jones L: *In vivo* methods for screening and preclinical testing. *In*: Anticancer Drug Development Guide. Teicher BA (ed.). Humana Press, Totowa, NJ, pp. 75-99, 1997.

Received March 8, 2011
Revised April 26, 2011
Accepted April 27, 2011